FIRST OBSERVATION AND BRANCHING FRACTION MEASUREMENT OF THE $\Lambda_b^0 \to D_s^- p$ DECAY*

Maciej Giza

on behalf of the LHCb Collaboration

H. Niewodniczański Institute of Nuclear Physics Polish Academy of Sciences
Radzikowskiego 152, 31-342 Kraków, Poland
maciej.artur.giza@cern.ch

Received 21 March 2023, accepted 18 April 2023, published online 6 September 2023

The first observation of the $\Lambda_b^0 \to D_s^- p$ decay is presented using proton–proton collision data collected by the LHCb experiment at a centre-of-mass energy of $\sqrt{s} = 13$ TeV, corresponding to a total integrated luminosity of $6\,\mathrm{fb}^{-1}$. Using the $\Lambda_b^0 \to \Lambda_c^+ \pi^-$ decay as the normalisation mode, the branching fraction of the $\Lambda_b^0 \to D_s^- p$ decay is measured to be $\mathcal{B}(\Lambda_b^0 \to D_s^- p) = (12.6 \pm 0.5 \pm 0.3 \pm 1.2) \times 10^{-6}$, where the first uncertainty is statistical, the second systematic, and the third due to uncertainties in the branching fractions of the $\Lambda_b^0 \to \Lambda_c^+ \pi^-$, $D_s^- \to K^- K^+ \pi^-$, and $\Lambda_c^+ \to p K^- \pi^+$ decays.

DOI:10.5506/APhysPolBSupp.16.7-A27

1. Introduction

In the Standard Model (SM) of particle physics, the Cabibbo–Kobayashi–Maskawa (CKM) mechanism describes how the weak interaction eigenstates are related to the mass eigenstates of the quarks and determines the interaction strengths among quarks via the weak interaction [1, 2]. The CKM-matrix element describing the $b \to u$ transition, V_{ub}, is the element with the smallest and most poorly determined magnitude. Better knowledge of $|V_{ub}|$ provides a valuable contribution for testing to check the consistency of the SM [3].

The $\Lambda_b^0 \to D_s^- p$ decay[1] is a weak hadronic decay that proceeds through a $b \to u$ transition. A single leading-order diagram contributes to this process, shown in Fig. 1. The $\Lambda_b^0 \to D_s^- p$ branching fraction is proportional to $|V_{ub}|^2$.

* Presented at the 29th Cracow Epiphany Conference on *Physics at the Electron–Ion Collider and Future Facilities*, Cracow, Poland, 16–19 January, 2023.

[1] Inclusion of charge-conjugated modes is implied unless explicitly stated.

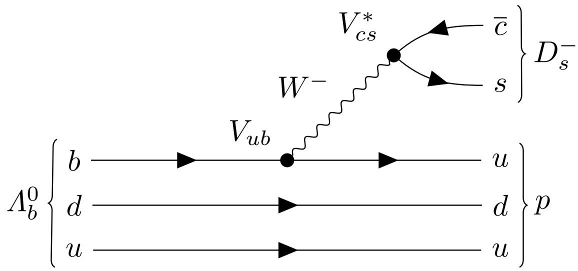

Fig. 1. Tree diagram contributing to the $\Lambda_b^0 \to D_s^- p$ decay.

Moreover, this measurement provides a measure to address the calculations of the branching fraction of the $B^0 \to D_s^+ \pi^-$ decay [4], which proceeds with the same tree-level transition as the $\Lambda_b^0 \to D_s^- p$ decay, leading to similar expression for the branching fraction, except for the form factor and nonfactorisable effects.

The paper [5] presents the first observation and branching fraction measurement of the $\Lambda_b^0 \to D_s^- p$ decay using proton–proton (pp) collision data collected with the LHCb detector at the centre-of-mass energy of 13 TeV and corresponding to an integrated luminosity of 6 fb^{-1}. The data taken in Run 2 of the Large Hadron Collider (LHC) between 2015 and 2018 are used. The $\Lambda_b^0 \to \Lambda_c^+ \pi^-$ decay is used as a normalisation channel because it is topologically similar to the signal decay and has a relatively high branching fraction. Candidates of $\Lambda_b^0 \to D_s^- p$ ($\Lambda_b^0 \to \Lambda_c^+ \pi^-$) decays are reconstructed using the final-state particles of the $D_s^- \to K^- K^+ \pi^-$ ($\Lambda_c^+ \to p K^- \pi^+$) decay. The branching fraction of $\Lambda_b^0 \to D_s^- p$ is determined using the following equation:

$$\mathcal{B}\left(\Lambda_b^0 \to D_s^- p\right) = \mathcal{B}\left(\Lambda_b^0 \to \Lambda_c^+ \pi^-\right) \frac{N_{\Lambda_b^0 \to D_s^- p}}{N_{\Lambda_b^0 \to \Lambda_c^+ \pi^-}} \frac{\epsilon_{\Lambda_b^0 \to \Lambda_c^+ \pi^-}}{\epsilon_{\Lambda_b^0 \to D_s^- p}} \frac{\mathcal{B}\left(\Lambda_c^+ \to p K^- \pi^+\right)}{\mathcal{B}\left(D_s^- \to K^- K^+ \pi^-\right)}\,, \tag{1}$$

where N_X is the measured yield of decay X and ϵ_X is the efficiency of the candidate reconstruction and selection.

2. Detector and simulation

The LHCb detector [6] is a single-arm forward spectrometer covering the pseudorapidity range of $2 < \eta < 5$, designed for the study of particles containing b or c quarks, *e.g.* via accessing the particle identification (PID) information with the help of two ring-imaging Cherenkov detectors. Simulations are required to calculate reconstruction and selection efficiencies, and to determine shapes of invariant-mass distributions. Toolkits such as PYTHIA [7] with a specific LHCb configuration [8], EvtGen [9], and Geant4 [10, 11], as described in Ref. [12], are used.

3. Selection of candidates

The $\Lambda_b^0 \to D_s^- p$ ($\Lambda_b^0 \to \Lambda_c^+ \pi^-$) decay is reconstructed by selecting $D_s^- \to K^- K^+ \pi^-$ ($\Lambda_c^+ \to p K^- \pi^+$) candidates and combining them with a proton (charged pion), which is referred to as the companion particle. Candidates that have been selected by the trigger requirements are subject to further offline selection to reduce the background contributions. The b-hadron and c-hadron candidates are preselected with good-quality vertices by reconstructing four well-reconstructed tracks with high transverse and total momentum and inconsistent with a hypothesis that it originates from any primary vertex (PV). The gradient-boosted decision tree (BDTG) algorithm [13, 14] is used to reduce the background contributions due to random combinations of final-state particles. This BDTG classifier is trained on $B_s^0 \to D_s^- \pi^+$ candidates taken in 2011 and 2012 (Run 1) and is described in Ref. [15]. The BDTG is suitable for decays topologically similar to $B_s^0 \to D_s^- \pi^+$, as it does not use particle identification variables. The classifier combines a number of track-related variables, including the transverse momentum of the companion particle, the b-hadron and c-hadron candidate's flight distance and the companion and b-hadron's minimum χ^2_{IP}, where χ^2_{IP} is defined as the difference in the vertex-fit χ^2 of the PV reconstructed with and without the candidate [16].

To separate $\Lambda_b^0 \to D_s^- p$ and $\Lambda_b^0 \to \Lambda_c^+ \pi^-$ from backgrounds with a misidentified final-state particles, requirements concerning the PID of the decay products of these signals are applied. The efficiencies of the candidate selection and the hardware trigger efficiency are calculated using calibration data samples and simulated decays [5]. Two control channels, $B_s^0 \to D_s^- \pi^+$ and $B_s^0 \to D_s^{\mp} K^{\pm}$, are used to estimate the contributions of misidentified $B_s^0 \to D_s^{(*)-}\{\pi^+, \rho^+\}$ and $B_{(s)}^0 \to D_s^{(*)\mp} K^{(*)\pm}$ decays in the $\Lambda_b^0 \to D_s^- p$ sample.

4. Invariant-mass fits

The yields of the signal $\Lambda_b^0 \to D_s^- p$ and normalisation $\Lambda_b^0 \to \Lambda_c^+ \pi^-$ channels are determined using unbinned maximum-likelihood fits to the $D_s^- p$ and $\Lambda_c^+ \pi^-$ invariant-mass distributions, respectively. The candidate samples from different years of data-taking and magnet polarities are combined in the fits. Parametrisations of the signal components are obtained from fits to samples of simulated candidates. The residual combinatorial background contribution is modelled using analytic functions. The background shapes are determined from simulation or described analytically [5].

Decays where one or more of the final-state particles are missed by the reconstruction are referred to as partially reconstructed backgrounds. These are the decays where a neutral pion or photon is not reconstructed. The fit to $\Lambda_b^0 \to D_s^- p$ candidates considers partially reconstructed background components from $\Lambda_b^0 \to D_s^{*-}(\to D_s^- \gamma/\pi^0)p$ decays. The $\Lambda_b^0 \to \Lambda_c^+ \pi^-$ sample contains partially reconstructed backgrounds from $\Lambda_b^0 \to \Lambda_c^+ \rho^-(\to \pi^- \pi^0)$ and $\Lambda_b^0 \to \Sigma_c^+(\to \Lambda_c^+ \pi^0)\pi^-$ decays. The yields of partially reconstructed background components are left free in the fits.

The background contributions due to the misidentification of the companion particle in the $m(D_s^- p)$ fit consist of the $B_s^0 \to D_s^- \pi^+$, $B_s^0 \to D_s^\mp K^\pm$, $B^0 \to D_s^- K^+$ decays and the corresponding backgrounds with missing photons or neutral pions in the final state, originating from $\rho^+ \to \pi^+ \pi^0$, $K^{*+} \to K^+ \pi^0$ or $D_s^{*-} \to D_s^- \{\gamma, \pi^0\}$ decays. Fits to the B_s^0 invariant mass in the $B_s^0 \to D_s^- \pi^+$ and $B_s^0 \to D_s^\mp K^\pm$ control samples provide an estimate of the contributions of the misidentified background components in the $\Lambda_b^0 \to D_s^- p$ sample. These estimates are computed by correcting the observed yields of $B_s^0 \to D_s^{(*)-}\{\pi^+, \rho^+\}$ and $B_{(s)}^0 \to D_s^{(*)\mp} K^{(*)\pm}$ decays for the different PID requirements between the control and signal samples. Subsequently, they are constrained in the $m(D_s^- p)$ fit.

The sample of $\Lambda_b^0 \to \Lambda_c^+ \pi^-$ candidates is contaminated by the $\Lambda_b^0 \to \Lambda_c^+ K^-$, $B_s^0 \to D_s^- \pi^+$, and $B^0 \to D^- \pi^+$ backgrounds due to the misidentification of one of the final-state particles. The size of the $\Lambda_b^0 \to \Lambda_c^+ K^-$ contribution is constrained to the expected yield determined using knowledge of its branching fraction and efficiencies obtained from simulation. A data-driven method is used to determine the $B_s^0 \to D_s^- \pi^+$ and $B^0 \to D^- \pi^+$ yields in the $m(\Lambda_c^+ \pi^-)$ fit. The $\Lambda_c^+ \pi^-$ data are reconstructed as $D_s^- \pi^+$ and $D^- \pi^+$, and the resulting yields are corrected for the difference in the PID and invariant-mass requirements. The expected number of $B_s^0 \to D_s^- \pi^+$ and $B^0 \to D^- \pi^+$ candidates is relatively small. Their yields are fixed in the fit to $\Lambda_b^0 \to \Lambda_c^+ \pi^-$ candidates.

The $\Lambda_c^+ \pi^-$ invariant-mass distribution and the fit projection of the $\Lambda_b^0 \to \Lambda_c^+ \pi^-$ signal and the background components are shown in Fig. 2. The $\Lambda_b^0 \to \Lambda_c^+ \pi^-$ yield obtained from this fit is $404\,700 \pm 700$ events, where the uncertainty is statistical. The fit to the invariant-mass distribution of the $\Lambda_b^0 \to D_s^- p$ candidates is shown in Fig. 3. A clear $\Lambda_b^0 \to D_s^- p$ signal peak is visible, corresponding to a yield of 831 ± 32 events, where the uncertainty is statistical. This result constitutes the first observation of this decay.

The fits to $\Lambda_b^0 \to D_s^- p$ and $\Lambda_b^0 \to \Lambda_c^+ \pi^-$ candidates are studied for stability and any bias on the signal yields using pseudoexperiments. They are found to be stable, without any sizeable biases. Furthermore, the fit is validated using the data samples split according to magnet polarity, year of data taking, BDTG response, and trigger decision.

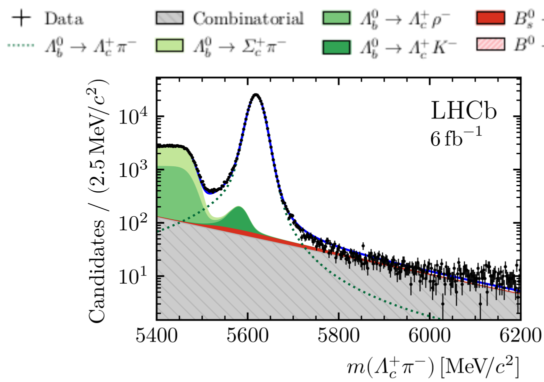

Fig. 2. Invariant-mass distribution of the $\Lambda_b^0 \to \Lambda_c^+ \pi^-$ candidates, the normalisation channel in logarithmic scale. Overlaid are the fit projections of the signal and background contributions, with individual components illustrated in the legend above [5].

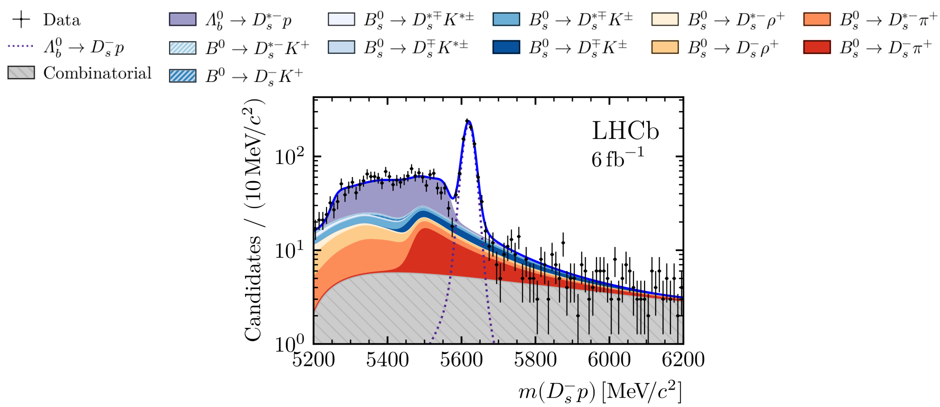

Fig. 3. Invariant-mass distribution of the $\Lambda_b^0 \to D_s^- p$ candidates, in logarithmic scale, where the fit projections of the signal and background contributions are overlaid. The individual components in the fit are illustrated in the legend [5].

Systematic uncertainties arising from the limited knowledge of the background and signal shapes, the expected background yields, and the PID and hardware trigger efficiencies are considered [5]. Due to similarities between the $\Lambda_b^0 \to D_s^- p$ and the $\Lambda_b^0 \to \Lambda_c^+ \pi^-$ decay topologies, many sources of systematic uncertainties either cancel or are suppressed. The total systematic uncertainty on the final branching fraction result is smaller than the statistical one and the uncertainties arising from the branching fraction inputs.

5. Results and conclusions

The branching fraction of $\Lambda_b^0 \to D_s^- p$ is determined using the efficiencies of the requirements described in Sec. 3 and the yields of the $\Lambda_b^0 \to D_s^- p$ and $\Lambda_b^0 \to \Lambda_c^+ \pi^-$ decays as obtained in Sec. 4. An external input for the $\Lambda_b^0 \to \Lambda_c^+ \pi^-$, $\Lambda_c^+ \to pK^-\pi^+$, and $D_s^- \to K^-K^+\pi^-$ branching fractions is given in Table 1.

Table 1. The obtained signal yields and efficiencies of the $\Lambda_b^0 \to D_s^- p$ and $\Lambda_b^0 \to \Lambda_c^+ \pi^-$ decays, as well as the branching fractions used for this measurement [17]. The uncertainty on the signal yields and efficiencies is statistical.

	$\Lambda_b^0 \to D_s^- p$	$\Lambda_b^0 \to \Lambda_c^+ \pi^-$
Yield	831 ± 32	$(4.047 \pm 0.007) \times 10^5$
Efficiency	$(0.1819 \pm 0.0013)\%$	$(0.1947 \pm 0.0012)\%$
$\mathcal{B}(\Lambda_b^0 \to \Lambda_c^+ \pi^-)$	$(4.9 \pm 0.4) \times 10^{-3}$	[17]
$\mathcal{B}(D_s^- \to K^-K^+\pi^-)$	$(5.38 \pm 0.10) \times 10^{-2}$	[17]
$\mathcal{B}(\Lambda_c^+ \to pK^-\pi^+)$	$(6.28 \pm 0.32) \times 10^{-2}$	[17]

The branching-fraction ratio of the $\Lambda_b^0 \to D_s^- p$ and $\Lambda_b^0 \to \Lambda_c^+ \pi^-$ decays is found to be

$$\frac{\mathcal{B}\left(\Lambda_b^0 \to D_s^- p\right)}{\mathcal{B}\left(\Lambda_b^0 \to \Lambda_c^+ \pi^-\right)} = (2.56 \pm 0.10 \pm 0.05 \pm 0.14) \times 10^{-3},$$

where the first uncertainty is statistical, the second systematic and the third due to the uncertainty on the $D_s^- \to K^-K^+\pi^-$ and $\Lambda_c^+ \to pK^-\pi^+$ branching fractions.

The branching fraction of the $\Lambda_b^0 \to D_s^- p$ decay is obtained to be

$$\mathcal{B}\left(\Lambda_b^0 \to D_s^- p\right) = (12.6 \pm 0.5 \pm 0.3 \pm 1.2) \times 10^{-6},$$

where the third uncertainty is due to the uncertainty on the $\Lambda_b^0 \to \Lambda_c^+ \pi^-$, $D_s^- \to K^-K^+\pi^-$ and $\Lambda_c^+ \to pK^-\pi^+$ branching fractions. This measurement is limited by the uncertainty on the $\Lambda_b^0 \to \Lambda_c^+ \pi^-$ branching fraction, which is dominated by the precision on the ratio of hadronisation fractions $f_{\Lambda_b^0}/f_d$.

In summary, the first observation of the $\Lambda_b^0 \to D_s^- p$ decay and its branching fraction measurement are reported. Additionally, the branching fraction ratio of the $\Lambda_b^0 \to D_s^- p$ and $\Lambda_b^0 \to \Lambda_c^+ \pi^-$ decays is determined. This measurement will serve as input for future studies of factorisation in hadronic Λ_b^0 decays.

REFERENCES

[1] N. Cabibbo, *Phys. Rev. Lett.* **10**, 531 (1963).

[2] M. Kobayashi, T. Maskawa, *Prog. Theor. Phys.* **49**, 652 (1973).

[3] UTfit Collaboration (M. Bona *et al.*), *J. High Energy Phys.* **10**, 081 (2006), updated results and plots available at `http://www.utfit.org/`

[4] LHCb Collaboration (R. Aaij *et al.*), *Eur. Phys. J. C* **81**, 314 (2021).

[5] LHCb Collaboration (R. Aaij *et al.*), *J. High Energy Phys.* **2023**, 75 (2023).

[6] LHCb Collaboration (A.A. Alves Jr. *et al.*), *J. Instrum.* **3**, S08005 (2008).

[7] T. Sjöstrand, S. Mrenna, P. Skands, *Comput. Phys. Commun.* **178**, 852 (2008).

[8] I. Belyaev *et al.*, *J. Phys.: Conf. Ser.* **331**, 032047 (2011).

[9] D.J. Lange, *Nucl. Instrum. Methods Phys. Res. A* **462**, 152 (2001).

[10] J. Allison *et al.*, *IEEE Trans. Nucl. Sci.* **53**, 270 (2006).

[11] S. Agostinelli *et al.*, *Nucl. Instrum. Methods Phys. Res. A* **506**, 250 (2003).

[12] M. Clemencic *et al.*, *J. Phys.: Conf. Ser.* **331**, 032023 (2011).

[13] L. Breiman, J.H. Friedman, R.A. Olshen, C.J. Stone, «Classification and Regression Trees», *Wadsworth International Group*, Belmont, California, USA 1984.

[14] B.P. Roe *et al.*, *Nucl. Instrum. Methods Phys. Res. A* **543**, 577 (2005).

[15] LHCb Collaboration (R. Aaij *et al.*), *J. High Energy Phys.* **2018**, 059 (2018).

[16] U.P. Eitschberger, Ph.D. Thesis, Technical University, Dortmund, 2018.

[17] Particle Data Group (R.L. Workman *et al.*), *Prog. Theor. Exp. Phys.* **2022**, 083C01 (2022).